

A Neuro-Fuzzy controller based Wind Generation System using Flying Supercapacitors

N. Swathi¹, M. Ramsekhar Reddy², M. Vijaya Kumar³

PG Student [PID], Dept. of EEE, JNTU College of Engineering, Ananthapuramu, Andhra Pradesh, India¹

Assistant Professor, Dept. of EEE, JNTU College of Engineering, Ananthapuramu, Andhra Pradesh, India²

Professor, Dept. of EEE, JNTU College of Engineering, Ananthapuramu, Andhra Pradesh, India³

ABSTRACT: This paper presents an approach of direct integration scheme for wind energy conversion systems using a capacitor-clamped three-level inverter-based supercapacitor. The main idea of this paper is to increase the capacitance of the clamping capacitors with the use of supercapacitors. The supercapacitor voltage is varied within a defined range. This variable voltage changes brings about many challenges. The uneven distribution of the space vector is the first challenge. To overcome this, space vector modulation technique is proposed. This generates undistorted currents even in the presence of dynamic changes in supercapacitor voltages. The harmonics are reduced by replacing conventional PI controllers with the Neuro-Fuzzy controllers which give better performance. The control strategies of the proposed system are discussed in detail. Simulation results are presented to study the efficacy of the proposed system in reducing wind power fluctuations.

KEYWORDS: Wind energy, Capacitor-clamped three-level inverter, Space Vector Modulation (SVM), Supercapacitor, Neuro-fuzzy controller.

I. INTRODUCTION

Usage of supercapacitors in wind power generation is drawing considerable attention presently. There are many techniques proposed in literature in this regard [1]-[4]. Depending on the way of the supercapacitor connection to the wind power system, these techniques are grouped into different schemes. In the first scheme, supercapacitors are connected to the dc link of the back-to-back converter system. This has drawbacks like limited voltage range and limited control over the power flow. This issue can be reduced if an intermediate dc-dc converter is placed between supercapacitor and the dc link [5], [6]. The second technique uses common ac bus for power exchange, and it requires an additional dc-dc converter, dc-ac inverter, and a coupling transformer. The aforementioned drawbacks are common for this configuration and could be alleviated if a direct integration scheme with full controllability is available. The third technique uses a dual-inverter structure for direct integration of supercapacitors, but this increases the cost and size of the system since two inverters are used.

To overcome the problems occur by the methods mentioned above, a direct integration scheme for supercapacitors using grid-side inverter is proposed. The approach looks like shown in Fig.1.

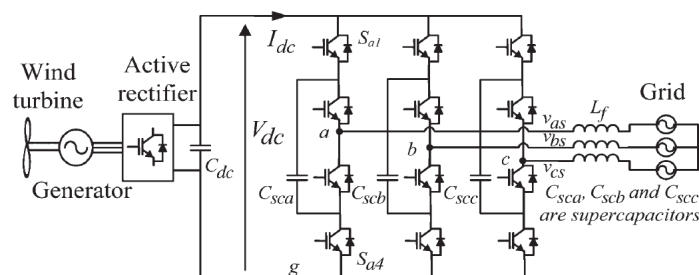


Fig. 1: Proposed capacitor-clamped three-level grid-side inverter-based super-capacitor direct integration scheme.

International Journal of Advanced Research in Electrical, Electronics and Instrumentation Engineering

(An ISO 3297: 2007 Certified Organization)

Vol. 4, Issue 7, July 2015

The capacities of the clamping capacitors are increased with the use of supercapacitors and these supercapacitor voltages are allowed to vary within safe operating region. This variable voltage operation gives rise to three major problems. The first issue is unequal blocking voltages and increased voltage slew rates (dv/dt) are experienced due to unbalanced voltages. For this purpose large band gap devices should be used. The second issue is unequal distribution of instantaneous power losses among switching devices. Heat sinks should be overrated to protect switching devices from thermal stresses. The third problem is uneven distribution of space vectors [7]. To tackle this issue Space Vector Modulation method is developed. In order to achieve supercapacitor voltage equalisation, a small vector selection-based controller, which controls the supercapacitor charging/discharging process, is proposed. Artificial intelligent techniques are now emerging as trend setting technology in many aspects of engineering which includes wind power systems [8]-[9]. A Neuro-fuzzy based controller is proposed instead of PI controllers to reduce the harmonics and to improve the wave quality of output voltage and current.

II. EFFECTS OF CAPACITOR VOLTAGE VARIATIONS

The supercapacitor voltage varies with its stored energy. Moreover, 50% reduction of supercapacitor voltage from the maximum value yields 75% discharge of the stored energy. The supercapacitor voltages are allowed to operate between 400 to 800V. The first step is to analyse the possible voltage levels in a capacitor-clamped three-level inverter. The line-to-ground voltage of each leg of the inverter can have maximum of four voltage levels. The corresponding gate signals, and switching states for the leg ‘a’ of the inverter is shown below in Table I. The other two legs also follow the same pattern.

TABLE I
SWITCHING STATES AND LINE-TO-GROUND VOLTAGES

Switching state (S_a)	Gate signals ($G_{a1}..G_{a4}$)	v_{ag}
0	0011	0
1	0101	V_{sca}
2	1010	$V_{dc} - V_{sca}$
3	1100	V_{dc}

If the supercapacitor voltages are balanced, the second and third voltage levels will be equal and total number of voltage levels will get reduced to three (0, $V_{dc}/2$, and V_{dc}). In this paper the space vectors of the flying-capacitor inverter system are classified into nine groups as shown in Table II.

TABLE II
VECTOR CLASSIFICATION

Large	Upper medium	Lower medium	Upper small 1	Upper small 2
003 030 033 300 303 330	023 032 203 230 302 320	013 031 103 130 301 310	113 131 133 311 313 331	223 232 233 322 323 332
Lower small 1	Lower small 2	Zero	Rest	
001 010 011 100 101 110	002 020 022 200 202 220	000 111 222 333	012 021 102 112 120 121 122 123 132 201 210 211 212 213 221 231 312 321	

III. MODULATION STRATEGY

Flying-capacitor converters operate at non-traditional voltage ratios. They use low –capacity electrolytic capacitors and therefore voltage balancing and regulation are possible within a short period of time. But, here supercapacitors are used which results in unequal and unbalanced capacitor voltage conditions. This paper presents SVM technique which

International Journal of Advanced Research in Electrical, Electronics and Instrumentation Engineering

(An ISO 3297: 2007 Certified Organization)

Vol. 4, Issue 7, July 2015

produces undistorted currents even under unbalanced and unequal voltage conditions. Block diagram of SVM technique is shown in Fig 2.

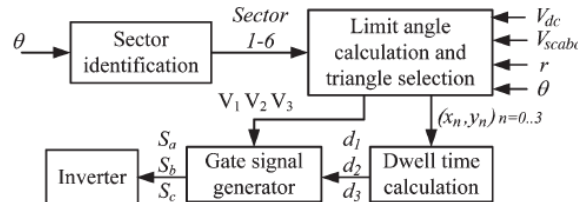


Fig. 2: Simplified block diagram of the proposed SVM technique

The amplitude r and the angle ϑ of the reference voltage vector are calculated using

$$r = \sqrt{v_d^{*2} + v_q^{*2}} \quad (1)$$

$$\theta = \tan^{-1} \left(\frac{v_q^*}{v_d^*} \right) + \theta_{\text{grid}} \quad (2)$$

Where v_d^* and v_q^* are d-q axis components of the reference voltage vector.

After finding the sector, find a triangle with three near vectors. This modulation strategy uses vectors in two hexagons at a time, i.e., vector in one of the inner hexagon and the outer hexagon. For a given reference vector, the number of candidate triangles is four. Due to these eight limit angles need to be calculated. For the simplicity of subsequent calculations, dc-side voltages are transformed into two variables x and y using

$$x = \frac{2}{3}(V_{\text{dc}} - V_{\text{sc}}) \quad y = \frac{2}{3}V_{\text{sc}} \quad (3)$$

Limit angles are calculated using the below equations, where α is an intermediate variable.

$$\alpha = \sin^{-1} \left(\frac{\sqrt{3}y}{2\sqrt{(x+y)^2 - 3xy}} \right) \quad (4)$$

Limit angles for other sectors can be derived from these angles with the help of Table III.

TABLE III
LIMIT ANGLES FOR SECTORS 1–6

Sector	θ_1^*	θ_2^*	θ_3^*	θ_4^*
1	θ_1	θ_2	θ_3	θ_4
2	$2\pi/3 - \theta_2$	$2\pi/3 - \theta_1$	$2\pi/3 - \theta_4$	$2\pi/3 - \theta_3$
3	$2\pi/3 + \theta_1$	$2\pi/3 + \theta_2$	$2\pi/3 + \theta_3$	$2\pi/3 + \theta_4$
4	$4\pi/3 - \theta_2$	$4\pi/3 - \theta_1$	$4\pi/3 - \theta_4$	$4\pi/3 - \theta_3$
5	$4\pi/3 + \theta_1$	$4\pi/3 + \theta_2$	$4\pi/3 + \theta_3$	$4\pi/3 + \theta_4$
6	$2\pi - \theta_2$	$2\pi - \theta_1$	$2\pi - \theta_4$	$2\pi - \theta_3$

After finding three vectors, the next time is to determine the switching times. These are represented as fractions of sampling time. The below equations are used to calculate the switching times.

$$\begin{aligned} \vec{V}_r &= d_1 \vec{V}_1 + d_2 \vec{V}_2 + d_3 \vec{V}_3 \\ d_1 + d_2 + d_3 &= 1 \end{aligned} \quad (5)$$

Where V_r is the reference vector and $V_1, V_2,$ and V_3 are the three adjacent vectors.

IV SUPERCAPACITOR VOLTAGE EQUALIZATION

The supercapacitor voltage equalization method is based on redundant state selection. Overlapping Small vectors provide these redundancies. For example small vectors (100,322) and (200,311) are redundant vector pairs as shown fig.3. Similarly there are ten redundant pairs attached to five sectors.

International Journal of Advanced Research in Electrical, Electronics and Instrumentation Engineering

(An ISO 3297: 2007 Certified Organization)

Vol. 4, Issue 7, July 2015

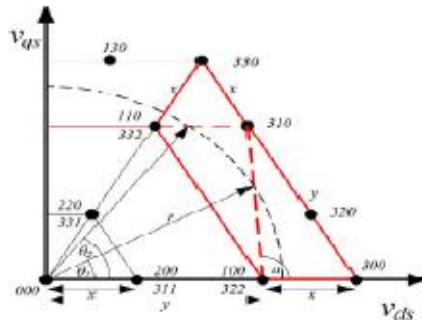


Fig 3: Limit angles for the sector 1

Half of the redundant pair vectors contribute to supercapacitor charging while the other half contribute to discharging of the supercapacitor. The block diagram is shown in Fig. 4.

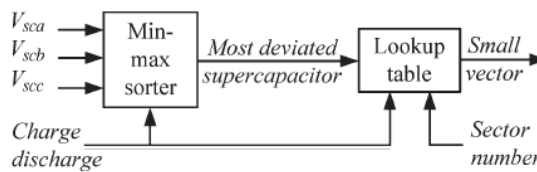


Fig 4: Block diagram of the supercapacitor voltage equalizer

Voltage equalizer measures supercapacitor voltages at every switching cycle and sorts them in the ascending order. The output of the minimum-maximum sorting block indicates the supercapacitor with highest deviation compared to the voltages of other two supercapacitors. In the charging condition, where supercapacitors are supposed to absorb power, the min-max sorter selects the supercapacitor with the lowest voltage as the deviated one and in the discharging condition, the min-max sorter selects the supercapacitor with the highest voltage as the most deviated one.

V. PROPOSED CONTROL STRATEGY

The proposed scheme is simulated using a permanent-magnet synchronous generator-based wind energy conversion system. The controller block diagram is shown below in Fig. 5. This controller consists of generator-side converter controller and grid-side inverter controller. The generated torque T_M is derived from the wind turbine model. The speed references for the generator are given from the wind speed, based on the optimal tip speed ratio of the wind turbine. The speed error is passed to the fuzzy logic control system instead of PI controller, which generates q-axis current component i_{qg}^* of the generator. The reference for the d-axis component is set to zero. These current references are compared with the actual currents and the errors are passed to the proposed controller to create voltage references for the subsequent modulation unit.

Similarly, the grid-side inverter controller is implemented in the synchronous reference frame where the d-axis current component i_d is varied in order to control the active power transfer to the grid. The q-axis current component is maintained at zero. These current references are compared with the actual currents and the errors are passed to the controller to create voltage references for the subsequent modulation unit.

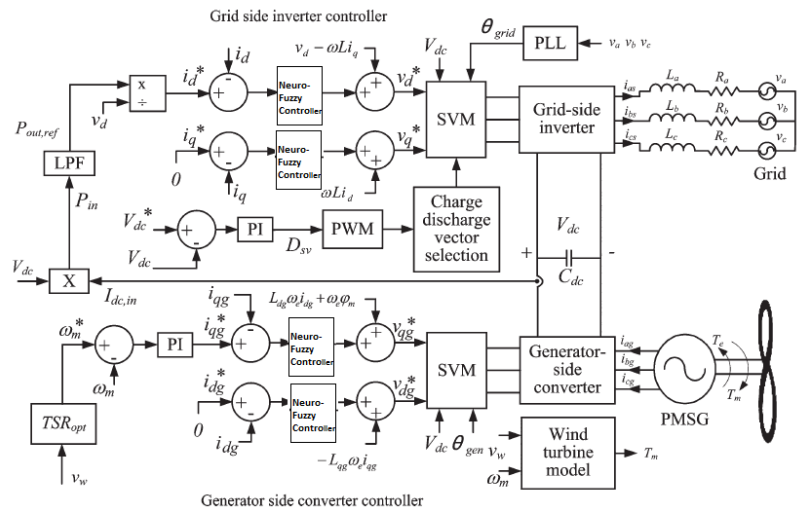


Fig.5: Controller block diagram of the inverter system.

The Simulink model of the controller block diagram is shown below in fig 6.

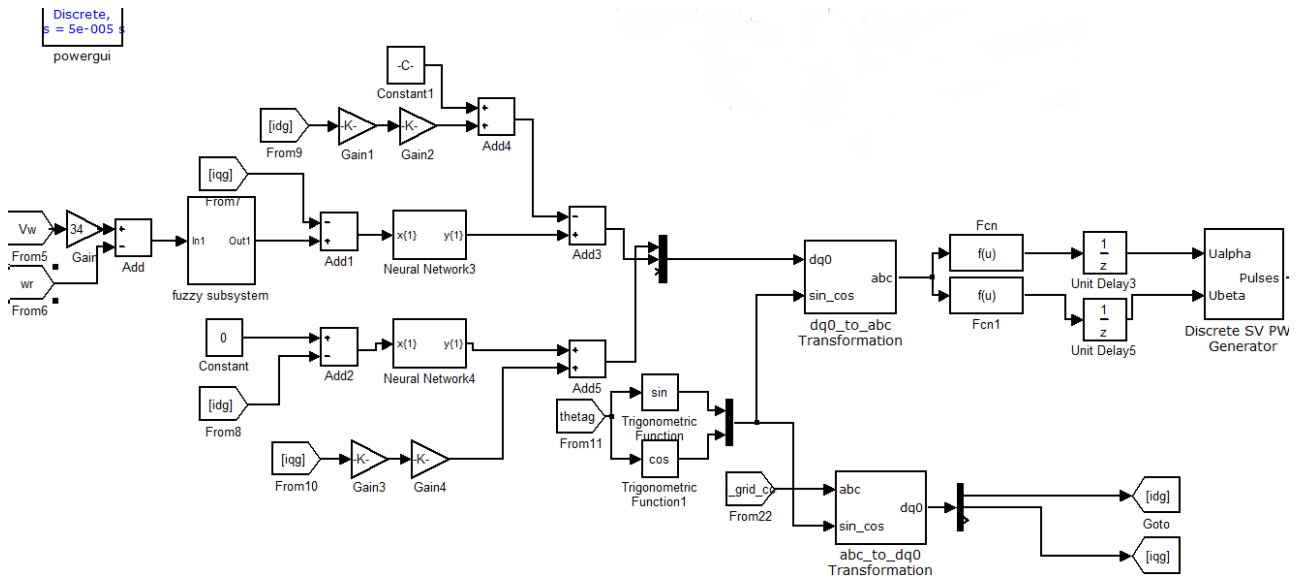


Fig. 6: Simulink model of the Controller for the proposed inverter system.

The power reference for the grid-side inverter controller is obtained by passing instantaneous output power of the generator side converter through a low-pass filter. If no other possibilities of energy storage are present, the residue of the instantaneous power is absorbed by the dc-link capacitor which in turn changes the dc-link voltage. In this system the supercapacitors are used to absorb the residue power and thus regulate the dc-link voltage. In the fuzzy logic controller 49 rules are framed using mamdani model. The GUI of the fuzzy inference system is as shown in Fig. The Neuro-Fuzzy control scheme is shown below in Fig.7.

International Journal of Advanced Research in Electrical, Electronics and Instrumentation Engineering

(An ISO 3297: 2007 Certified Organization)

Vol. 4, Issue 7, July 2015

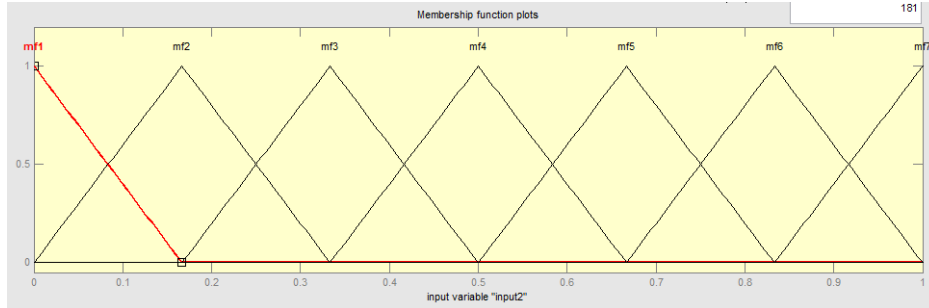


Fig.7 Membership functions of the fuzzy controller.

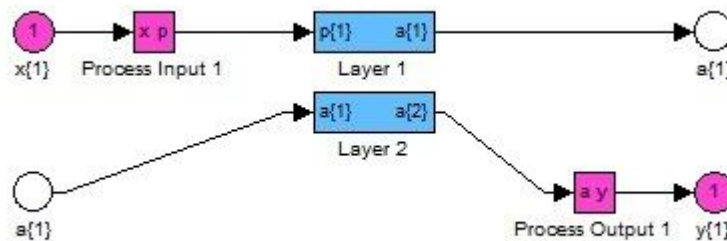


Fig.7: Simulink model control scheme of artificial neural network

VI. SIMULATION RESULTS

The performance of the proposed scheme has been studied using computer simulations on MATLAB/SIMULINK platform. The variations of the captured wind power P_{in} , output grid power P_{out} and supercapacitor power are shown in below fig 8.

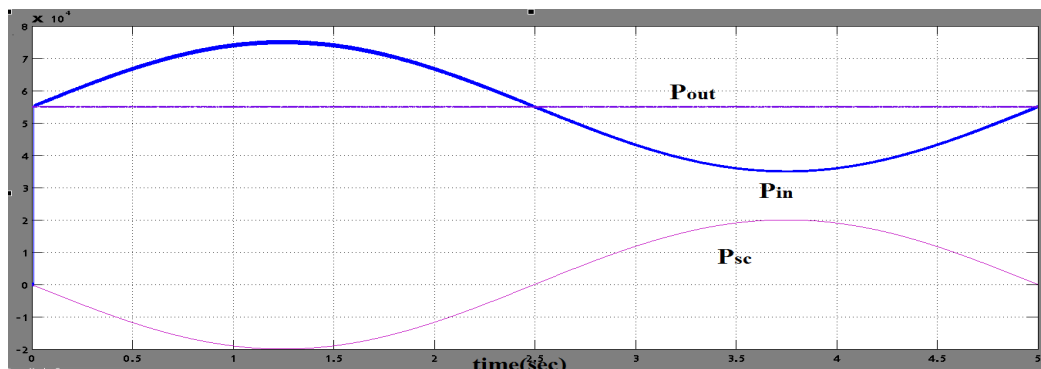


Fig 8: Input, Output and Supercapacitor powers

From Fig.8 it is evident that the output power P_{out} is free from the fluctuation present in the input power. The dc-link voltage is also well regulated since the supercapacitors of the grid-side inverter absorb the fluctuation present in the input power as shown.

When PI controller is used, the variations of the control signal for charge/discharge vector selection, inverter output voltage and inverter output current are shown below in fig 9.

International Journal of Advanced Research in Electrical, Electronics and Instrumentation Engineering

(An ISO 3297: 2007 Certified Organization)

Vol. 4, Issue 7, July 2015

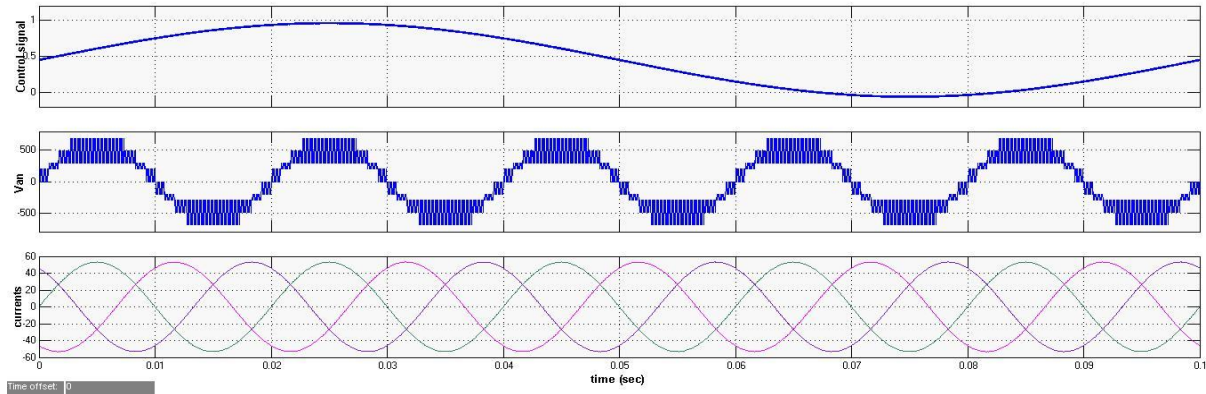


Fig 9: Control signal, inverter output voltage and currents

The supercapacitor voltages vary, while the dc-link voltage remains constant. This creates an imbalance in the flying-capacitor inverter, and thus, space vectors get distributed unevenly. The capability of the proposed modulation strategy in generating desired outputs even under such situations is proven by the results shown in Fig.9. The FFT analysis of the inverter output currents is shown below in fig 10.

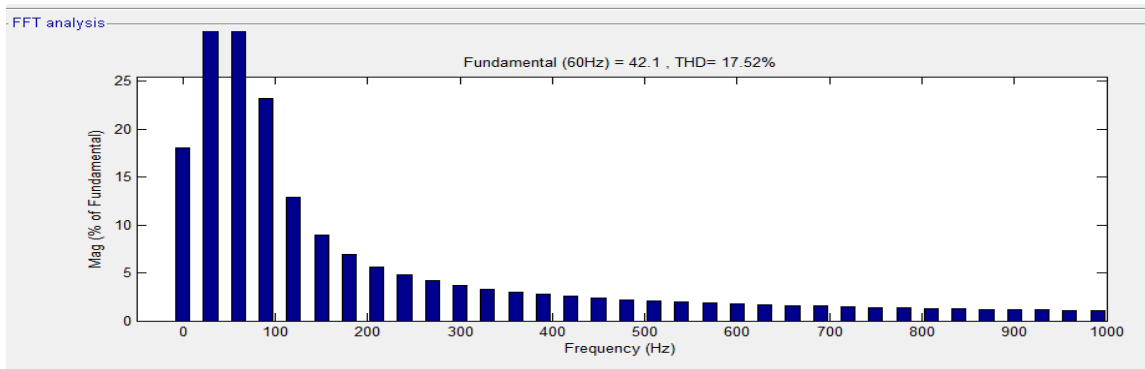


Fig 10: FFT analysis of inverter output current.

The desired output currents are produced under unbalanced and unequal voltage conditions. The total harmonic distortion value is 17.52% when PI controller is implemented.

When neuro-fuzzy controller is used the simulation results are shown below in Fig 11.

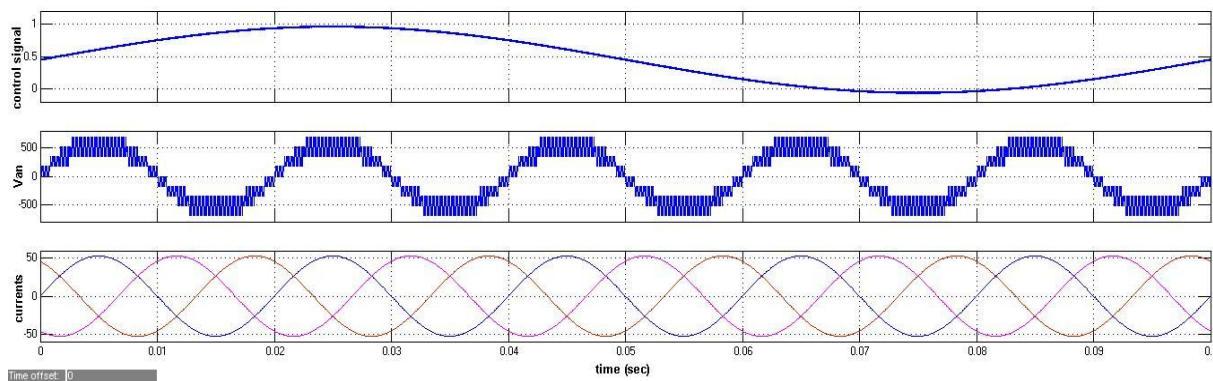


Fig 11: Control signal, inverter output voltage and currents

International Journal of Advanced Research in Electrical, Electronics and Instrumentation Engineering

(An ISO 3297: 2007 Certified Organization)

Vol. 4, Issue 7, July 2015

The harmonic distortion in voltage and current are very low compared to the outputs of fig 9. The FFT analysis for the inverter output current is shown below in fig 12.

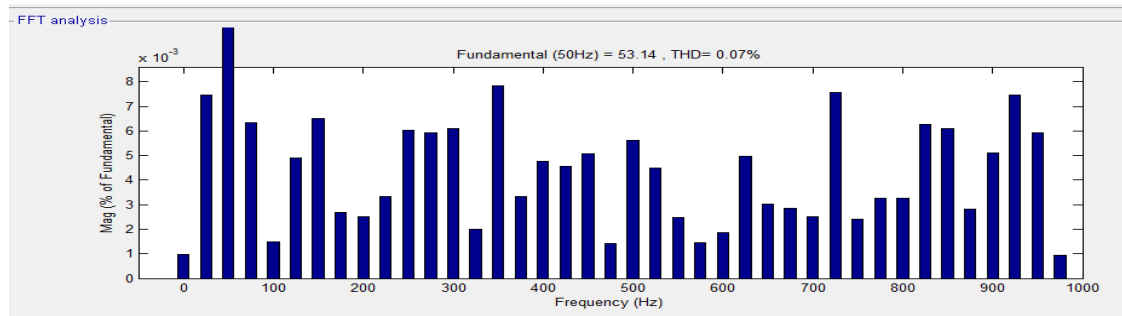


Fig 12: FFT analysis of inverter output current

The total harmonic distortion value is 0.07%. Figures 10 and 12 show that the harmonics are reduced and the efficacy of the output power is increased.

VI.CONCLUSION

In this paper, neuro-fuzzy implementation of a capacitor-clamped three-level grid-side inverter-based supercapacitor direct integration scheme has been proposed for mitigating the short term power fluctuations in wind energy conversion systems. The proposed Space vector modulation technique is used to generate desired outputs even in the presence of unequal and unbalanced voltages. A small-vector based controller is proposed to control the supercapacitor charging/discharging process. Neuro-fuzzy based controllers are implemented instead of PI controllers to get better performance. There is a decrease in the total harmonic distortion value and thus the efficacy of the system is increased.

REFERENCES

- [1] S. Jayasinghe and D. Vilathgamuwa "Flying supercapacitors as power smoothing elements in wind generation", IEEE Trans. Ind. Electron., vol. 60, no. 7, pp.2909-2918 2013.
- [2] T. H. Nguyen, D. C. Lee, S. Seung-Ho, and E. H. Kim, "Improvement of power quality for PMSG wind turbine systems," in Proc. IEEE ECCE, Sep. 12–16, 2010, pp. 2763–2770.
- [3] S. M. Mueen, R. Takahashi, T. Murata, and J. Tamura, "Integration of an energy capacitor system with a variable-speed wind generator," IEEE Trans. Energy Convers., vol. 24, no. 3, pp. 740–749, Sep. 2009.
- [4] B. Singh and G.K Kasal. "Voltage and frequency controller for a small scale wind power generation", in Asian Power Electronics Journal, Vol. 2, No. 1, Apr 2008, pp. 37-44.
- [5] S. R. Pulikanti and V. G. Agelidis, "Hybrid flying-capacitor-based active-neutral-point-clamped five-level converter operated with SHE-PWM," IEEE Trans. Ind. Electron., vol. 58, no. 10, pp. 4643–4653, Oct. 2011.
- [6] P. Lezana, P. Aguilera, and D. E. Quevedo, "Model predictive control of an asymmetric flying capacitor converter," IEEE Trans. Ind. Electron., vol. 56, no. 6, pp. 1839–1846, Jun. 2009.
- [7] D.O. Neacsu, "Space vector modulation-An introduction," in Proceedings of The 27th Annual Conference of the IEEE Industrial Electronics Society, IECON, 2001, vol.1, pp.1583-1592.
- [8] M. G. Simoes, B. K. Bose, and R. J. Spiegel, "Fuzzy logic-based intelligent control of a variable speed cage machine wind generation system," IEEE Trans. Power Electron. PE-12, 87–94 (1997).
- [9] H. Li, K. L. Shi, and P. G. McLaren, "Neural-network-based sensorless maximum wind energy capture with compensated power coefficient," IEEE Trans. Ind. Appl. 41(6), 1548–1556 (2005).